Available online at www.sciencedirect.com
ScienceDirect
Journal of Sound and Vibration 302 (2007) 903–924
JOURNAL OF SOUND AND VIBRATION
www.elsevier.com/locate/jsvi

Natural frequencies and mode shapes of deterministic and stochastic non-homogeneous rods and beams

Sarig Nachum, Eli Altus*

Faculty of Mechanical Engineering, Technion, Israel Institute of Technology, Haifa 32000, Israel

Received 8 March 2006; received in revised form 10 December 2006; accepted 18 December 2006
Available online 20 February 2007

Abstract

Natural frequencies and mode shapes of non-homogeneous (deterministic and stochastic) rods and beams are studied. The solution is based on the functional perturbation method (FPM). The frequencies and mode shapes are considered as functionals of the non-homogeneous properties. The natural frequency and mode shape of the kth order is obtained analytically to any desired degree of accuracy. Once the functional derivatives (with respect to the non-uniform property) have been found, the solution for any morphology is obtained by direct integration without resolving the differential equation. Several examples with different non-homogeneous properties are solved and compared with exact solutions as an accuracy check. The FPM accuracy range for the frequency ω and the mode shape is less than 1% even for high heterogeneities. In the stochastic case the accuracy of the natural frequencies depends on the stochastic information used/given, on the correlation distance (roughly the "grain size"), on the function around which the perturbation is executed, and on whether we are interested in the properties of ω or of ω^2. Moreover, all frequency modes have the same response to heterogeneity as long as their wave length is of the order of the heterogeneity's characteristic distance. In addition, the heterogeneity effect on the average natural frequencies is minimal for the fundamental mode, and may serve as a design tool.

1. Introduction and motivation

Many practical applications require knowledge of the natural frequencies and mode shapes of rods and beams with non-uniform material and geometrical properties, such as Young's modulus E or compliance S, the cross section A or inertia I, and the density ρ. Their variation can be deterministic or stochastic. Where this variation is random, the natural frequencies and mode shapes are random too. Different methods – exact and approximate – for finding the natural frequencies are available in literature. Exact solutions exist only for limited cases of non-uniformity and serve as a benchmark for the approximate ones. Analytical solutions, albeit approximate, are important for physical insight.

A wide variety of studies are available on this subject, but only a few will be mentioned here. Eisenberger [1] studied the vibration of (deterministic) tapered rods, Aberate [2] found exact solutions for rods and beams

*Corresponding author. Fax: 972 4 8295711.
E-mail addresses: sarign@tx.technion.ac.il (S. Nachum), altus@tx.technion.ac.il (E. Altus).

0022-460X/$ - see front matter © 2007 Elsevier Ltd. All rights reserved.
doi:10.1016/j.jsv.2006.12.021

with polynomial cross sections and inertia. For the same non-uniformities in rods, Kumar and Sujith [3] used suitable transformations and obtained results in terms of Bessel and Neumann functions. Horgan and Chan [4] obtained exact solutions for polynomial and exponential variations of strings, rods and membranes. Elishakoff et al. [5] and Elishakoff and Candan [6] used the inverse method and obtained the exact natural frequencies in rods and beams with polynomially varying material and geometrical properties. In the stochastic case, Hoshiya and Shah [7] studied the free vibration of beams. They used the perturbation method and obtained a mean value of the natural frequency identical to that in the deterministic free vibration case. Recently, Ganesan and Kowda [8] studied the free vibration of composite beams. They used the same procedure as Hoshiya and Shah [7] by taking only the first-order terms and obtained the same result for the mean value. The current study will show the difference when more terms are taken into account. Vaicaitis [9] considered the free vibration of beams with random characteristic and applied a two-variable perturbation expansion, which necessitated formulation of a new problem involving slowly varying non-uniformity. Again, only the first-order terms were taken into account. Manohar and Keane [10] studied the vibration of stochastic rods and obtained an exact solution for a specific combination of system parameters.

In this study the natural frequencies and mode shapes of the kth-order of non-homogeneous (deterministic and stochastic) rods and beams are found. The solution is based on the functional perturbation method (FPM), recently developed for bending, strength and buckling [11–13]. It permits solution of boundary value problems with non-homogeneous properties. It is based on considering the unknown field variables (such as frequencies and mode shapes) as functionals of the non-homogeneous properties. The FPM is applied directly to the governing equation by functionally expanding the frequency and the mode shape in Frèchet series. The unknown functional derivatives of the frequency and mode shape are then obtained by means of the Fredholm Theorem and the Green Function associated with the homogenous equation. Once the functional derivatives have been found, the solution for any morphology is obtained by direct integration without re-solving the differential equation for each heterogeneity. In this sense the functional derivatives serve as "Green Functions of morphology". The solutions are analytical, and therefore give a physical insight into the effect of the heterogeneity of each frequency order.

Using a second-order solution, the FPM results are compared with exact solutions and its accuracy is examined. The same functional derivatives are applied for the stochastic problems, when the average and variance of the kth-order frequency are found analytically.

2. Mathematical notations

Some basic mathematical and statistical notations are introduced. For conciseness, we write:

$$U(x) \equiv U_x, \quad \frac{\mathrm{d}U(x)}{\mathrm{d}x} \equiv U_{x,x}, \quad \frac{\mathrm{d}^2U(x)}{\mathrm{d}x^2} \equiv U_{x,xx}, \text{etc.} \tag{1}$$

If U is also a functional of θ, while θ is a function of x_1, the first functional derivative of U with respect to θ_{x1} reads [14]:

$$\frac{\delta U(x,\{\theta_x\})}{\delta\theta_1} \equiv U_{x,\theta_1}, \tag{2}$$

where $(),_{\theta 1}$ stands for $(),_{\theta x1}$ etc. The notation $\{\}$ denotes a functional relation and the derivative Eq. (2) is a functional of θ and a function of both x and x_1. Similarly, the second functional derivative reads:

$$\frac{\delta^2 U(x,\{\theta_x\})}{\delta\theta x_2 \delta\theta x_1} \equiv U_{x,\theta_1\theta_2}, \text{etc.} \tag{3}$$

The Dirac operator will be used frequently in the text. Its differential definition is especially convenient [14]:

$$\delta(x - x_1) = \delta_{xx_1} = \frac{\delta\theta_x}{\delta\theta_{x_1}}. \tag{4}$$

The Dirac derivative is denoted similarly:

$$\frac{\delta(\theta_{x,x})}{\delta\theta_{x1}} = \left(\frac{\delta\theta_x}{\delta\theta_{x1}}\right)_{,x} = \delta_{xx_1,x}. \tag{5}$$

Notice the symmetry relations:

$$\delta_{xx_1} = \delta_{x_1x}, \quad \delta_{xx_1,x} = -\delta_{xx_1,x_1}. \tag{6}$$

Integrations are denoted by the convolution sign. For example, the x integration of U_{x_1x} with f_{xx_2} is:

$$\int_0^1 U_{x_1x} f_{xx_2} dx = U_{x_1x} \underset{x=0}{\overset{1}{*}} f_{xx_2}. \tag{7}$$

Since [0,1] are the convolution intervals in this study, we write concisely:

$$\int_0^1 U_{x_1x} f_{xx_2} \mathrm{d}x = U_{x_1x} * f_{xx_2}. \tag{8}$$

Let θ_x be a stochastic function which describes some property of the rod or beam. Denote $\langle\theta\rangle$, θ'_x and $\bar{\theta}'_x$ as the statistical average, deviation and normalization (usually to some average value) of θ, respectively:

$$\theta'_x = \theta_x - \langle\theta\rangle, \quad \bar{\theta}_x = \frac{\theta_x}{\langle\theta\rangle}, \quad \bar{\theta}'_x = \frac{\theta_x - \langle\theta\rangle}{\langle\theta\rangle}. \tag{9}$$

3. Problem formulation

3.1. Longitudinally vibrating rods

The longitudinal free motion of a rod of length L, with varying cross-section A_x, density ρ_x and elastic modulus E_x is governed by the differential equation [15]:

$$\left(A_xE_xu_{xt,x}\right)_{,x} = \rho_xA_xu_{xt,tt}. \tag{10}$$

Assuming a particular solution of the form:

$$u_{xt} = U_xT_t, \tag{11}$$

and substituting in Eq. (10), we obtain two uncoupled differential equations:

$$T_{t,tt} + \omega^2T_t = 0, \tag{12}$$

$$\left(E_xA_xU_{x,x}\right)_{,x} + L^2\rho_xA_x\omega^2U_x = 0, \tag{13}$$

where x in Eq. (13) is an axial coordinate normalized to the rod's length (L), U_x the mode shape and ω the natural frequency. As an example, consider a rod with non-homogeneity E_x only. Consequently, Eq. (13) reduces to:

$$J(x, U\{E\}, \omega\{E\}) = E_{x,x}U_{x,x} + E_xU_{x,xx} + \rho L^2\omega^2U_x = 0. \tag{14}$$

Eq. (14) is a linear differential equation with non-uniform coefficients, presenting an operator J which is a function of x and a functional of E through both U and ω. The mode shapes and natural frequencies are considered as functionals of the morphology E, since any change in E at some x_1 obviously affects U and ω. Expanding functionally the natural frequency and the mode shape in a Frèchet series of increasing order, we have:

$$\omega(\{E\}) = \omega(\langle E\rangle) + \omega_{,E_1}\big|_{\langle E\rangle} * E'_1 + \frac{1}{2}\omega_{,E_1E_2}\bigg|_{\langle E\rangle} * * E'_1E'_2 + \cdots, \tag{15}$$

$$U(x, \{E\}) = U(\langle E\rangle) + U_{,E_1}\big|_{\langle E\rangle} * E'_1 + \frac{1}{2}U_{,E_1E_2}\bigg|_{\langle E\rangle} * * E'_1E'_2 + \cdots, \tag{16}$$

where all functional derivatives are calculated at $\langle E\rangle$. Using Eq. (9) and the shifting property of the Dirac operator, we can also write:

$$E'_x = \delta_{xx_1} * E'_1. \tag{17}$$

Our goal is to find the two series Eqs. (15) and (16), from which we calculate the natural frequencies and mode shapes. Expansion of J functionally about $\langle E\rangle$ leads to the series:

$$J(x,\{E\}) = J(\langle E\rangle) + J_{,E_1}\big|_{\langle E\rangle} * E'_1 + \frac{1}{2}J_{,E_1E_2}\bigg|_{\langle E\rangle} * *E'_1E'_2 + \cdots = 0. \tag{18}$$

Since J vanishes for any heterogeneity E'_x, all its derivatives vanish too, which leads to a set of successive linear differential equations with constant coefficients:

$$J(\langle E\rangle) = 0, \quad J_{,E_1}\big|_{\langle E\rangle} = 0, \quad J_{,E_1E_2}\big|_{\langle E\rangle} = 0. \tag{19}$$

The first term (zero order) of Eq. (19) is the case where $E = \langle E\rangle$ meaning a homogeneous rod, which yields:

$$J(\langle E\rangle) = U^{(0)}_{x,xx} + \beta^2 U^{(0)}_x = 0, \quad \beta^2 = \frac{L^2\rho\left(\omega^{(0)}\right)^2}{\langle E\rangle}. \tag{20}$$

$U_x{}^{(0)}$ and $\omega^{(0)}$ are the mode shapes and natural frequencies for the homogeneous rod. For later convenience, we choose to normalize Eq. (15) to $\omega^{(0)}$:

$$\bar{\omega}(\{E\}) = \frac{\omega(\{E\})}{\omega^{(0)}} = 1 + \bar{\omega}_{,E_1} * E'_1 + \frac{1}{2}\bar{\omega}_{,E_1E_2} * *E'_1E'_2 + \cdots, \tag{21}$$

and $U_x{}^{(0)}$ such that:

$$\left(U^{(0)}_x\right)^2 * 1_x = 1. \tag{22}$$

Using the notation of Section 2, the first functional derivative of J is:

$$\frac{\delta J}{\delta E x_1} = J_{,E_1} = \begin{pmatrix} \delta_{xx_1}U_{x,xx} + E_xU_{x,xxE_1} + \delta_{xx_1,x}U_{x,x} \\ +E_{x,x}U_{x,xE_1} + \rho L^2\omega^2 U_{x,E_1} + 2\rho L^2\omega\omega_{,E_1}U_x \end{pmatrix} = 0. \tag{23}$$

Substitution of $\langle E\rangle$ and rearranging leads to:

$$U^{(1)}_{xx_1,xx} + \beta^2 U^{(1)}_{xx_1} = f^{(1)}_{xx_1}, \tag{24}$$

where

$$U^{(1)}_{xx_1} \equiv U_{x,E_1}\big|_{\langle E\rangle}, \quad \omega^{(1)}_{x_1} \equiv \omega_{,E_1}\big|_{\langle E\rangle}, \tag{25}$$

$$f^{(1)}_{xx_1} = -\frac{1}{\langle E\rangle}\left(\delta_{xx_1}U^{(0)}_{x,xx} + \delta_{xx_1,x}U^{(0)}_{x,x} + 2\rho L^2\omega^{(0)}\omega^{(1)}_{x_1}U^{(0)}_x\right). \tag{26}$$

Eq. (24) is a non-homogeneous linear differential equation for $U^{(1)}_{xx_1}$ (first functional derivative of U). The left-hand part is identical to the homogeneous equation and the right-hand part contains known functions of x ($U^{(0)}_x, \delta_{xx_1}$ and their derivatives), and the unknown function of x_1 ($\omega^{(1)}_{x_1}$). Following Fredholm's Theorem [16], Eq. (24) has a non-trivial solution if and only if:

$$f^{(1)}_{xx_1} * U^{(0)}_x = 0. \tag{27}$$

Using Eqs. (27) and (22), $\omega^{(1)}_{x_1}$ can be extracted as:

$$\bar{\omega}^{(1)}_{x_1} = \frac{\left(U^{(0)}_{x_1,x_1}\right)^2}{2\langle E\rangle\beta^2}. \tag{28}$$

Evidently, Eq. (28) depends on "homogeneous terms" only and is independent of the heterogeneous morphology. Hence, the second term in the frequency series Eq. (21) can be found by integrating Eq. (28) with

respect to E_1':

$$\omega_{x_1}^{(1)} * E_1'. \tag{29}$$

To solve Eq. (24), $f_{xx_1}^{(1)}$ is convoluted with the Green Function associated with the homogeneous equation (Eq. (20)). The Green Function is obtainable whenever an exact solution for the homogeneous case is available. The Modified Green Function is used here [17], which is continuous and satisfies the consistency condition, the rod's boundary conditions and the equation:

$$G_{x\xi,xx} + \beta^2 G_{x\xi} = \delta_{x\xi} - U_x^{(0)} U_\xi^{(0)}. \tag{30}$$

The coordinate ξ is a point along the rod where the singular load is applied. Solving Eq. (30) yields G with an arbitrary constant. Choosing a particular modified Green Function such that:

$$G_{x\xi} * U_x^{(0)} = 0, \tag{31}$$

we have in addition a symmetric G with respect to its variables (x,ξ). Thus, using Eq. (22) and the condition (31), the solution for Eq. (24) is:

$$U_{xx_1}^{(1)} = G_{x\xi} * f_{\xi x_1}^{(1)} = \frac{U_{x_1,x_1}^{(0)} G_{x_1,x,x_1}}{\langle E \rangle}. \tag{32}$$

The second term in Eq. (16) is therefore:

$$U_{xx_1}^{(1)} * E_1'. \tag{33}$$

The second functional derivative of J is:

$$\frac{\delta^2 J}{\delta E_{x_2} \delta E_{x_1}} = J_{,E_1E_2} \left(\begin{array}{l} 2\delta_{xx_1} U_{x,xxE_2} + E_x U_{x,xxE_1E_2} \\ +2\delta_{xx_1,x} U_{x,xE_2} + E_{x,x} U_{x,xE_1E_2} \\ +\rho L^2 \left(\begin{array}{l} 4\omega\omega_{,E_1} U_{x,E_2} + \omega^2 U_{x,E_1E_2} \\ +2\omega_{,E_1}\omega_{,E_2} U_x + 2\omega\omega_{,E_1E_2} U_x \end{array} \right) \end{array} \right) = 0. \tag{34}$$

Substituting $\langle E \rangle$ in Eq. (34) and rearranging we have:

$$U_{xx_1x_2,xx}^{(2)} + \beta^2 U_{xx_1x_2}^{(2)} = f_{xx_1x_2}^{(2)}, \tag{35}$$

where

$$U_{xx_1x_2}^{(2)} \equiv \tfrac{1}{2} U_{x,E_1E_2}\Big|_{\langle E \rangle}, \quad \omega_{x_1x_2}^{(2)} \equiv \frac{1}{2}\omega_{,E_1E_2}\Big|_{\langle E \rangle}, \tag{36}$$

$$f_{xx_1x_2}^{(2)} = -\frac{1}{\langle E \rangle} \left(\begin{array}{l} \delta_{xx_1} U_{xx_2,xx}^{(1)} + \delta_{xx_1,x} U_{xx_2,x}^{(1)} \\ +\rho L^2 \left(\begin{array}{l} 2\omega^{(0)}\omega_{x_1}^{(1)} U_{xx_2}^{(1)} + \omega_{x_1}^{(1)}\omega_{x_2}^{(1)} U_x^{(0)} \\ +2\omega^{(0)}\omega_{x_1x_2}^{(2)} U_x^{(0)} \end{array} \right) \end{array} \right) = 0. \tag{37}$$

In order to find $\omega_{x_1x_2}^{(2)}$ we use again the Fredholm Theorem:

$$f_{xx_1x_2}^{(2)} * U_x^{(0)} = 0. \tag{38}$$

Using Eqs. (38) and (22) we obtain:

$$\bar{\omega}_{x_1x_2}^{(2)} = \frac{1}{2} \left(\frac{U_{x_1x_2,x_1}^{(1)} U_{x_1,x_1}^{(0)}}{\langle E \rangle \beta^2} - \bar{\omega}_{x_1}^{(1)} \bar{\omega}_{x_2}^{(1)} \right). \tag{39}$$

Substitution of Eqs. (28) and (32) in Eq. (39) yields finally:

$$\bar{\omega}^{(2)}_{x_1x_2} = \frac{U^{(0)}_{x_2,x_2} U^{(0)}_{x_1,x_1}}{8\langle E\rangle^2\beta^2}\left(4G_{x_2x_1,x_2x_1} - \frac{U^{(0)}_{x_2,x_2} U^{(0)}_{x_1,x_1}}{\beta^2}\right). \tag{40}$$

The third term in Eq. (21) can be found by integrating Eq. (40) with respect to $E'_1E'_2$:

$$\omega^{(2)}_{x_1x_2} * *E'_1E'_2. \tag{41}$$

Convoluting $f^{(2)}_{xx_1x_2}$ with the Green Function calculated once for the first perturbation order, the solution for Eq. (35) is obtained as:

$$U^{(2)}_{xx_1x_2} = G_{\xi x} \underset{\xi=0}{\overset{1}{*}} f^{(2)}_{\xi x_1x_2} = \frac{1}{\langle E\rangle}\begin{pmatrix} G_{x_1x,x_2} U^{(1)}_{x_1x_2,x_1} \\ -2\beta^2\langle E\rangle\bar{\omega}^{(1)}_{x_1}\left(G_{x\xi} * U^{(1)}_{\xi x_2}\right)\end{pmatrix}. \tag{42}$$

Substitution of Eqs. (28) and (32) in Eq. (42) yields the final term:

$$U^{(2)}_{xx_1x_2} = \frac{U^{(0)}_{x_2,x_2}}{\langle E\rangle^2}\left(G_{x_1x,x_2}G_{x_2x_1,x_2x_1} - 2U^{(0)}_{x_1,x_1}\left(G_{x\xi} * G_{\xi x_2}\right)_{,x_2}\right). \tag{43}$$

The third term for the mode shape series Eq. (16) will be:

$$U^{(2)}_{xx_1x_2} * *E'_1E'_2. \tag{44}$$

It can be seen that the functional derivatives of the ω and U depend on homogeneous solutions and are independent of the heterogeneous morphology. Furthermore, these derivatives are generic results of solving each order perturbation and do not depend on prescribed shape functions. Therefore, the solution for any morphology is obtained by integrating the derivatives with respect to the relevant heterogeneity. In this sense the functional derivatives serve as "Green Functions of morphology". Once the functional derivatives (with respect to the non-uniform property) have been found, the solution for any morphology is obtained by direct integration without re-solving the differential equation for each type of heterogeneity separately.

3.2. Transversely vibrating beams

The static equation of a transversely vibrating beam with length L, stiffness $K_x = EI_x$ and mass per unit length m_x is governed by the following differential equation [15]:

$$\left(K_xU_{x,xx}\right)_{,xx} - \omega^2L^4m_xU_x = 0, \tag{45}$$

where x in Eq. (45) is an axial coordinate normalized to the beam's length (L), U_x is the mode shape and ω the natural frequency. Let J be an operator such that:

$$J(x, U\{K,m\}, \omega\{K,m\}) = \left(\bar{K}_xU_{x,xx}\right)_{,xx} - \beta^4\bar{\omega}^2\bar{m}_xU_x = 0, \tag{46}$$

where

$$\bar{K}_x = \frac{K_x}{\langle K\rangle}, \quad \bar{m}_x = \frac{m_x}{\langle m\rangle}, \quad \bar{\omega} = \frac{\omega}{\omega^{(0)}}, \quad \beta^4 = \frac{\langle m\rangle L^4\left(\omega^{(0)}\right)^2}{\langle K\rangle}. \tag{47}$$

For simpler notation, denote the vector $\mathbf{v}$:

$$\mathbf{v}'^i_x = \begin{Bmatrix} K'_x \\ m'_x\end{Bmatrix}, \quad \langle\mathbf{v}\rangle = \begin{Bmatrix}\langle K\rangle \\ \langle m\rangle\end{Bmatrix}, \quad i = 1,2. \tag{48}$$

Expansion of J functionally about $\langle\mathbf{v}\rangle$ leads to the series:

$$J(x,\{\mathbf{v}\}) = J(\langle\mathbf{v}\rangle) + J_{,\mathbf{v}^i_1}\Big|_{\langle\mathbf{v}\rangle} * \mathbf{v}'^i_1 + \frac{1}{2}J_{,\mathbf{v}^i_1\mathbf{v}^j_2}\Big|_{\langle\mathbf{v}\rangle} * *\mathbf{v}'^i_1\mathbf{v}'^j_2 + \cdots = 0. \tag{49}$$

Since J vanishes for any $\mathbf{v}'_x$, all its derivatives vanish too, which leads to a set of successive linear differential equations with constant coefficients:

$$J(\langle \mathbf{v} \rangle) = 0, \quad J_{,\mathbf{v}_1^i}\Big|_{\langle \mathbf{v} \rangle} = 0, \quad J_{,\mathbf{v}_1^i \mathbf{v}_2^j}\Big|_{\langle \mathbf{v} \rangle} = 0. \tag{50}$$

The first term (zero order) of equation Eq. (50) is the homogeneous beam where $\mathbf{v} = \langle \mathbf{v} \rangle$, which yields:

$$J(\langle \mathbf{v} \rangle) = U^{(0)}_{x,xxxx} - \beta^4 U^{(0)}_x = 0. \tag{51}$$

$U_x{}^{(0)}$ and $\omega^{(0)}$ are the mode shapes and natural frequencies for the homogeneous beam. Expanding functionally the natural frequency and the mode shape as a Frèchet about $\langle \mathbf{v} \rangle$, we have:

$$\bar{\omega}(\{\mathbf{v}\}) = \frac{\omega(\{\mathbf{v}\})}{\omega^{(0)}} = 1 + \bar{\omega}_{,\mathbf{v}_1^i}\Big|_{\langle \mathbf{v} \rangle} * \mathbf{v}'^i_1 + \frac{1}{2}\bar{\omega}_{,\mathbf{v}_1^i \mathbf{v}_2^j}\Big|_{\langle \mathbf{v} \rangle} * * \mathbf{v}'^i_1 \mathbf{v}'^j_2 + \cdots, \tag{52}$$

$$U(x, \{\mathbf{v}\}) = U(\langle \mathbf{v} \rangle) + U_{,\mathbf{v}_1^i} * \mathbf{v}'^i_1 + \frac{1}{2} U_{,\mathbf{v}_1^i \mathbf{v}_2^j} * * \mathbf{v}'^i_1 \mathbf{v}'^j_2 + \cdots. \tag{53}$$

For later convenience, we choose to normalize $U_x{}^{(0)}$ to:

$$\left(U^{(0)}_x\right)^2 * 1_x = 1. \tag{54}$$

The first functional derivative of J is:

$$\frac{\delta J}{\delta \mathbf{v}^i_{x_1}} = J_{,\mathbf{v}_1^i} = \left\{ \begin{array}{l} \left(\bar{K}_x U_{x,xx}\right)_{,xxK_1} - \beta^4 \bar{m}_x \left(\bar{\omega}^2 U_x\right)_{,K_1} \\ \bar{K}_x \left(U_{x,xx}\right)_{,xxm_1} - \beta^4 \left(\bar{m}_x \bar{\omega}^2 U_x\right)_{,m_1} \end{array} \right\} = 0. \tag{55}$$

Substitution of $\langle \mathbf{v} \rangle$ in Eq. (55) and rearranging leads to:

$$U^{(1)}_{x\mathbf{v}_1^i,xxxx} - \beta^4 U^{(1)}_{x\mathbf{v}_1^i} = f^{(1)}_{x\mathbf{v}_1^i}, \tag{56}$$

where

$$U^{(1)}_{x\mathbf{v}_1^i} \equiv U_{x,\mathbf{v}_1^i}\Big|_{\langle \mathbf{v} \rangle} = \left\{ \begin{array}{l} U_{x,K_1} \\ U_{x,m_1} \end{array} \right\}\Big|_{\langle \mathbf{v} \rangle}, \quad \omega^{(1)}_{\mathbf{v}_1^i} \equiv \omega_{,\mathbf{v}_1^i}\Big|_{\langle \mathbf{v} \rangle} \left\{ \begin{array}{l} \omega_{,K_1} \\ \omega_{,m_1} \end{array} \right\}\Big|_{\langle \mathbf{v} \rangle}, \tag{57}$$

$$f^{(1)}_{x\mathbf{v}_1^i} = \left\{ \begin{array}{l} 2\beta^4 \bar{\omega}^{(1)}_{\mathbf{v}_1^1} U^{(0)}_x - \left(\delta_{xx_1} U^{(0)}_{x,xx}\right)_{,xx} \Big/ \langle K \rangle \\ \beta^4 U^{(0)}_x \left(\delta_{xx_1} \Big/ \langle m \rangle + 2\bar{\omega}^{(1)}_{\mathbf{v}_1^2}\right) \end{array} \right\}. \tag{58}$$

Following the Fredholm Theorem, $\omega^{(1)}_{\mathbf{v}_1}$ can be extracted as:

$$\bar{\omega}^{(1)}_{\mathbf{v}_1^i} = \frac{1}{2} \left\{ \begin{array}{l} \left(U^{(0)}_{x_1,x_1x_1}\right)^2 \Big/ \beta^4 \langle K \rangle \\ -\left(U^{(0)}_{x_1}\right)^2 \Big/ \langle m \rangle \end{array} \right\}. \tag{59}$$

To solve Eq. (56), $f^{(1)}_{x\mathbf{v}_1}$ is convoluted with the Green Function associated with the beam's homogeneous equation (Eq. (51)) . Thus, the solution of Eq. (56) is:

$$U^{(1)}_{x\mathbf{v}_1^i} = G_{x\xi} * f^{(1)}_{\xi\mathbf{v}_1^i} = \left\{ \begin{array}{l} -U^{(0)}_{x_1,x_1x_1} G_{x_1x,x_1x_1} \Big/ \langle K \rangle \\ \beta^4 U^{(0)}_{x_1} G_{x_1x} \Big/ \langle m \rangle \end{array} \right\}. \tag{60}$$

The second functional derivative of J is:

$$J_{,\mathbf{v}_1^1\mathbf{v}_2^1} = \left(\bar{K}_x U_{x,xx}\right)_{,xxK_1K_2} - \beta^4 \bar{m}_x \left(\bar{\omega}^2 U_x\right)_{,K_1K_2}, \tag{61}$$

$$J_{,\mathbf{v}_1^2\mathbf{v}_2^2} = \bar{K}_x U_{x,xxm_1m_2} - \beta^4 \left(\bar{m}_x \bar{\omega}^2 U_x\right)_{,m_1m_2}, \tag{62}$$

$$J_{,\mathbf{v}_1^1\mathbf{v}_2^2} = \left(\bar{K}_x U_{x.xx}\right)_{,xxK_1m_2} - \beta^4 \left(\bar{m}_x \bar{\omega}^2 U_x\right)_{,K_1m_2}. \tag{63}$$

Substitution of $\langle \mathbf{v} \rangle$ in Eqs. (61)–(63) and rearranging yields:

$$U^{(2)}_{x\mathbf{v}_1^i\mathbf{v}_2^j,xxxx} - \beta^4 U^{(2)}_{x\mathbf{v}_1^i\mathbf{v}_2^j} = f^{(2)}_{x\mathbf{v}_1^i\mathbf{v}_2^j}, \tag{64}$$

where

$$U^{(2)}_{x\mathbf{v}_1^i\mathbf{v}_2^j} \equiv \frac{1}{2} U_{x,\mathbf{v}_1^i\mathbf{v}_2^j}\Big|_{\langle \mathbf{v} \rangle}, \quad \omega^{(2)}_{\mathbf{v}_1^i\mathbf{v}_2^j} \equiv \frac{1}{2} \omega_{,\mathbf{v}_1^i\mathbf{v}_2^j}\Big|_{\langle \mathbf{v} \rangle}, \tag{65}$$

$$f^{(2)}_{x\mathbf{v}_1^1\mathbf{v}_2^1} = \left(-\frac{1}{\langle K \rangle} \left(\delta_{xx_1} U^{(1)}_{x\mathbf{v}_2^1,xx} \right)_{,xx} + \beta^4 \left(\begin{array}{l} 2\bar{\omega}^{(1)}_{\mathbf{v}_1^1} U^{(1)}_{x\mathbf{v}_2^1} + \bar{\omega}^{(1)}_{\mathbf{v}_1^1} \bar{\omega}^{(1)}_{\mathbf{v}_2^1} U^{(0)}_x \\ +2\bar{\omega}^{(2)}_{\mathbf{v}_1^1\mathbf{v}_2^1} U^{(0)}_x \end{array} \right) \right), \tag{66}$$

$$f^{(2)}_{x\mathbf{v}_1^2\mathbf{v}_2^2} = \beta^4 \left(\begin{array}{l} U^{(0)}_x \left(2\delta_{xx_1} \bar{\omega}^{(1)}_{\mathbf{v}_2^2} \Big/ \langle m \rangle + \bar{\omega}^{(1)}_{\mathbf{v}_1^2} \bar{\omega}^{(1)}_{\mathbf{v}_2^2} + 2\bar{\omega}^{(2)}_{\mathbf{v}_1^2\mathbf{v}_2^2} \right) \\ + \left(\delta_{xx_1} / \langle m \rangle + 2\bar{\omega}^{(1)}_{\mathbf{v}_1^2} \right) U^{(1)}_{x\mathbf{v}_2^2} \end{array} \right), \tag{67}$$

$$f^{(2)}_{x\mathbf{v}_1^1\mathbf{v}_2^2} = \left(\begin{array}{l} \left(\delta_{xx_1} U^{(1)}_{x\mathbf{v}_2^2,xx} \right)_{,xx} \Big/ 2\langle K \rangle - \beta^4 \left(2\omega^{(1)}_{\mathbf{v}_1^1} U^{(1)}_{x\mathbf{v}_2^2} + \delta_{xx_1} U^{(1)}_{x\mathbf{v}_2^1} \Big/ \langle m \rangle \right) \\ -\beta^4 U^{(0)}_x \left(\delta_{xx_1} \bar{\omega}^{(1)}_{\mathbf{v}_2^1} \Big/ \langle m \rangle + \bar{\omega}^{(1,k)}_{\mathbf{v}_1^1} \bar{\omega}^{(1)}_{\mathbf{v}_2^2} + 2\bar{\omega}^{(2)}_{\mathbf{v}_1^1\mathbf{v}_2^2} \right) \end{array} \right). \tag{68}$$

Using the Fredholm Theorem and Eqs. (59)–(60), the second functional derivatives of ω can be extracted:

$$\omega^{(2)}_{\mathbf{v}_1^1\mathbf{v}_2^1} = -\frac{U^{(0)}_{x_1,x_1x_1} U^{(0)}_{x_2,x_2x_2}}{8\beta^8 \langle K \rangle^2} \left(\begin{array}{l} 4\beta^4 G_{x_2x_1,x_2x_2x_1x_1} \\ +U^{(0)}_{x_1,x_1x_1} U^{(0)}_{x_2,x_2x_2} \end{array} \right), \tag{69}$$

$$\omega^{(2)}_{\mathbf{v}_1^2\mathbf{v}_2^2} = \frac{U^{(0)}_{x_1} U^{(0)}_{x_2}}{8\langle m \rangle^2} \left(4\beta^4 G_{x_2x_1} - 3U^{(0)}_{x_1} U^{(0)}_{x_2} \right), \tag{70}$$

$$\omega^{(2)}_{\mathbf{v}_1^1\mathbf{v}_2^2} = \frac{U^{(0)}_{x_2} U^{(0)}_{x_1,x_1x_1} \beta^4}{4\langle K \rangle \langle m \rangle} \left(U^{(0)}_{x_2} U^{(0)}_{x_1,x_1x_1} \Big/ \beta^4 - 3G_{x_2x_1,x_1x_1} \right). \tag{71}$$

Using the Green Function calculated for the first perturbation order, the solution for the second functional derivative of U is obtained as:

$$U^{(2)}_{x\mathbf{v}_1^1\mathbf{v}_2^1} = \frac{U^{(0)}_{x_2,x_2x_2}}{2\langle K\rangle^2}\begin{pmatrix} G_{x_1x,x_1x_1}G_{x_2x_1,x_2x_2x_1x_1} \\ -\left(U^{(0)}_{x_1,x_1x_1}\right)^2\left(G_{\xi x} * G_{x_2\xi,x_2x_2}\right)\end{pmatrix}, \tag{72}$$

$$U^{(2)}_{x\mathbf{v}_1^2\mathbf{v}_2^2} = \frac{\beta^4 U^{(0)}_{x_2}}{\langle m\rangle^2}\left(\beta^4\begin{pmatrix}\left(G_{x_1x}G_{x_2x_1}\right) \\ -\left(U^{(0)}_{x_1}\right)^2\left(G_{\xi x} * G_{x_2\xi}\right)\end{pmatrix} - U^{(0)}_{x_2}U^{(0)}_{x_1}G_{x_1x}\right), \tag{73}$$

$$U^{(2)}_{x\mathbf{v}_1^1\mathbf{v}_2^2} = \frac{U^{(0)}_{x_2}}{\langle K\rangle\langle m\rangle}\begin{pmatrix}\left(U^{(0)}_{x_1,x_1x_1}\right)^2 G_{x_2x}\Big/2 \\ +\begin{pmatrix} G_{x_1x,x_1x_1}\beta^4 G_{x_2x_1,x_1x_1} \\ -\beta^4\left(U^{(0)}_{x_1,x_1x_1}\right)^2\left(G_{\xi x} * G_{x_2\xi}\right)\end{pmatrix}\end{pmatrix}. \tag{74}$$

4. The deterministic case

In this section, the FPM solutions for the natural frequencies and mode shapes of rods and beams with varying material and geometrical properties are compared with exact solutions for some particular cases. All comparisons are up to the second-order approximation, namely:

$$\omega_{\mathrm{FPM}} = \omega^{(0)} + \omega^{(1)}_{x_1} * \theta'_1 + \omega^{(2)}_{x_1x_2} * *\theta'_1\theta'_2, \tag{75}$$

$$U_{\mathrm{FPM}} = U^{(0)}_{x} + U^{(1)}_{xx_1} * \theta'_1 + U^{(2)}_{xx_1x_2} * *\theta'_1\theta'_2, \tag{76}$$

where θ is the non-uniform property. In addition, all functional derivatives are calculated at $\langle\theta\rangle$, defined as:

$$\langle\theta\rangle = \theta_x * 1. \tag{77}$$

In the deterministic case Eq. (77) is only one way of defining $\langle\theta\rangle$. For our comparison we use the relative error measures as:

$$\mathrm{Error}(U) = \sqrt{\frac{(U_x - U_{\mathrm{FPM}})^2 * 1_x}{U_x^2 * 1_x}}, \quad \mathrm{Error}(\omega) = \left|\frac{\omega_{\mathrm{exact}} - \omega_{\mathrm{FPM}}}{\omega_{\mathrm{exact}}}\right|. \tag{78}$$

Elishakoff [5] found exact solutions for particular cases by the inverse method, namely, finding E_x and ω such that the mode shape is a pre-selected function. Postulating U_x and E_x for a clamped–clamped (C–C) rod as:

$$U_x = x - 3x^2 + 2x^3, \quad E_x = 3\langle E\rangle\left(\frac{1}{6} + x - x^2\right), \tag{79}$$

where x is an axial coordinate normalized to L, the exact frequency reads:

$$\omega_{\mathrm{exact}} = \frac{1}{L}\sqrt{\frac{12}{\rho}}. \tag{80}$$

Using the homogeneous values of a C–C rod (see Appendix A, Eqs. (A.1) and (A.2)) we calculate the functional derivatives of ω (Eqs. (28) and (40)). Then, integrating the first and second functional derivatives with respect to E'_1 and $E'_1E'_2$, respectively, we obtain:

$$\omega_{\mathrm{FPM}} = \frac{45 - 135(k\pi)^2 + 157(k\pi)^4}{160\sqrt{3}(k\pi)^3 L\sqrt{\rho}}, \tag{81}$$

where k is the mode number. Setting $k=2$ in Eq. (81) for the second mode shape, we obtain:

$$\text{Error}(\omega)=0.537\%,\quad \text{Error}(U)=1.16\%. \tag{82}$$

For a non-homogeneous beam, Elishakoff and Candan [6] found again, by the inverse method, closed-form solutions to the dynamic response of a beam in which E_x is polynomial. For a simply-supported (S–S) beam where U_x and E_x are:

$$U_x=x-2x^3+x^4,\quad E_x=\frac{15}{53}\langle E\rangle\left(3+3x-2x^2-2x^3+x^4\right), \tag{83}$$

the exact fundamental frequency is:

$$\omega_{\text{exact}}=\frac{1}{L}\sqrt{\frac{360}{\rho}}. \tag{84}$$

Using the homogeneous values of an S–S beam (Eqs. (A.5) and (A.6)) we calculate the functional derivatives of ω (Eqs. (59) and (69)). Then, integrating the first and second functional derivatives with respect to E'_1 and $E'_1E'_2$, respectively, the FPM result for $k=1$ is:

$$\omega_{\text{FPM}}=\frac{1}{23744\sqrt{795}\pi^6L\sqrt{\rho}}\begin{pmatrix}255150+486675\pi^2+369495\pi^4+324285\pi^6\\+1256542\pi^8-226800\pi^5\tanh\left(\frac{\pi}{2}\right)\end{pmatrix}. \tag{85}$$

The relative error for the natural frequency in this case is 0.0011%.

In addition to its high accuracy, the FPM yields solutions for *any* mode number—in contrast to the method of Refs. [5,6], where new calculations are needed in order to obtain solutions for higher frequencies. Moreover, change of the boundary conditions or of E_x in the FPM does not necessitate re-solving the problem again. All that is need is to convolute the new morphology deviation with the functional derivatives calculated under the new boundary conditions. For example, for a clamped free (C–F) rod with:

$$U_x=x-\frac{x}{2},\quad E_x=\frac{3}{8}\langle E\rangle\left(2+2x-x^2\right), \tag{86}$$

the exact fundamental frequency is:

$$\omega_{\text{exact}}=\frac{1}{L}\sqrt{\frac{6}{\rho}}. \tag{87}$$

Calculating the same functional derivatives of ω (Eqs. (28) and (40)) using the homogeneous values of C–F rod (Eqs. (A.3) and (A.4)), we obtain:

$$\omega_{\text{FPM}}=\frac{1}{51840\pi^6L\sqrt{\rho}}\begin{pmatrix}-4675840+4186880\pi-1326245\pi^2\\+70560\pi^3+2580\pi^4+51948\pi^6\end{pmatrix}. \tag{88}$$

The relative error for the natural frequency in this case is $\text{Error}(\omega)=0.372\%$.

Table 1
Relative error between the exact and FPM natural frequencies for a non-homogeneous C–C rod with variations $A_x=\sin^2(1+x)$ and $A_x=(1+x)^4$

	$A_x=\sin^2(1+x)$			$A_x=(1+x)^4$		
Mode	ω_{Exact}	ω_{FPM}	Error (ω) %	ω_{Exact}	ω_{FPM}	Error (ω) %
1	2.9781	2.9791	0.0324	3.1334	3.2456	3.58
2	6.203	6.2039	0.013	6.2789	6.2863	0.119
3	9.3715	9.3724	0.009	9.4219	9.4198	0.0217
4	12.5265	12.5273	0.005	12.5642	12.5608	0.0273
5	15.6761	15.6767	0.004	15.7062	15.7028	0.022
6	18.823	18.8236	0.002	18.8481	18.8449	0.017

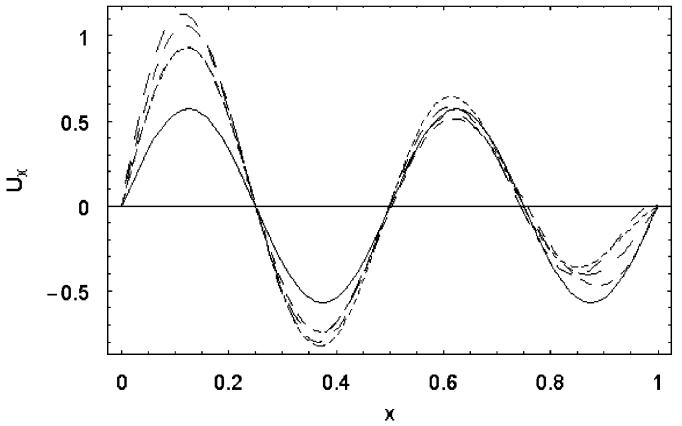

Fig. 1. Exact mode shape and zero, first and second-order FPM mode shapes for a non-homogeneous C–C rod with $A_x = (1+x)^4$: ——, zero order: - - - - -, first order: – – – –, second order: — —, exact.

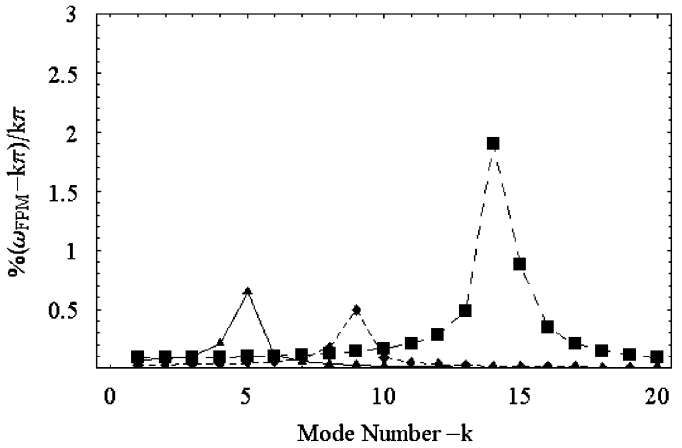

Fig. 2. Response of the FPM natural frequency for a non-homogeneous C–C rod Eq. (89) relative to the corresponding homogeneous one Vs. mode number. Note that α corresponds to wave length heterogeneity: —▲—, $\alpha = 30$: - - - - ◆ - - - -, $\alpha = 55$: —■—, $\alpha = 90$.

Kumar and Sujith [3] used appropriate transformations to Eq. (13) with varying cross-section and constant ρ and E. Analytical solutions were obtained for polynomial and sinusoidal variations in terms of Bessel and Neumann functions. Table 1 shows the frequency relative error between the exact and FPM results for the first 6 modes, for the variations $A_x = \sin^2(1+x)$ and $A_x = (1+x)^4$. Although the last variation changes sixteen times between the endpoints, this example also shows good convergence. It can be seen that since the wave length of this particular heterogeneity is of the order of one, the first mode is the most affected relative to the homogeneous frequency. Fig. 1 shows the convergence between the FPM and exact mode shapes corresponding to the fourth natural frequency. It was found that for this case the FPM zero-order term starts with Error$(U) = 47\%$ and reaches Error$(U) = 9\%$ when using three terms. This example demonstrates that even for large deviations the FPM converges rapidly to the exact solution as higher orders are considered.

In order to obtain insight into the effect of heterogeneity on the frequency modes consider the variation of E in a C–C rod:

$$E_x = 1 + 0.1\sin(1 + \alpha x), \tag{89}$$

where α is a non-dimensional parameter which controls the wave length of the heterogeneity. Fig. 2 shows the response of the FPM non-homogeneous natural frequency (calculated up to the second order), relative to its homogeneous counterpart. It is seen that the strongest response corresponds to the mode with wave length

equal to the heterogeneity's characteristic distance. For example, when $\alpha = 30$ the heterogeneity wave length equals 5, consequently the strongest response is obtained in the fifth mode. This result demonstrates the possibility of identifying heterogeneity by its sensitivity to high frequency modes. The same effect is found in the stochastic case as well.

5. The stochastic case

The strong advantage of the FPM is the ability to find for an unknown property (here, natural frequencies) analytical solutions of statistical characteristics such as the mean and variance. The processes for finding these values for a C–C rod and an S–S beam with a spatially varying modulus are demonstrated and the results examined (more complicated boundary conditions can be treated similarly). Then, some results for cross section variation in C–C rods are presented and discussed.

It is assumed that the random field is statistically homogeneous, therefore:

$$\langle \theta_x \rangle \equiv \langle \theta \rangle = \text{Constant}. \tag{90}$$

The variance and normalized variance of θ_x are:

$$\sigma_\theta^2 = \left\langle \left(\theta'_x\right)^2 \right\rangle = \langle (\theta_x)^2 \rangle - \langle \theta \rangle^2, \quad \bar{\sigma}_\theta^2 = \frac{\sigma_\theta^2}{\langle \theta \rangle^2}. \tag{91}$$

For a statistically homogeneous morphology, the two-point correlation function of θ is defined as:

$$\left\langle \theta'_{x_1} \theta'_{x_2} \right\rangle = \left\langle \theta'_{x_1} \theta'_{(x_1+h)} \right\rangle = \left\langle \theta'_{x_1} \theta'_{(x_1-h)} \right\rangle, \tag{92}$$

where x_1 and x_2 are normalized axial coordinates (to L), and h is the absolute distance between them. We define an effective "correlation length (distance)" λ as:

$$\int_0^\infty \left\langle \theta'_x \theta'_{(x+h)} \right\rangle \mathrm{d}h = \lambda \left\langle \left(\theta'_x\right)^2 \right\rangle = \lambda \sigma_\theta^2, \tag{93}$$

which is the normalized spacing (to L) of a pair of points beyond which the correlation in θ is small. In grainy materials, λ is linearly related to the average grain size. It is also relevant to other areas of analysis that will be described later. The above definition of λ is not unique, and other "sizes" can be defined. A convenient correlation function commonly used has an exponential form:

$$\langle \theta'_{x_1} \theta'_{x_2} \rangle = \sigma_\theta^2 \exp\left(-\frac{h}{\lambda}\right) = \sigma_\theta^2 \exp\left(\frac{|x_2 - x_1|}{\lambda}\right). \tag{94}$$

Although the FPM is not restricted to this shape only, Eq. (94) will be used throughout.

5.1. Modulus variation in rods and beams

We consider E as a statistically homogeneous random field with mean $\langle E \rangle$ and variance $\sigma^2{}_E$. Averaging Eq. (15), using the equality $\langle E' \rangle = 0$ and rearranging, an analytical expression for the natural frequency mean is obtained as:

$$\langle \omega \rangle = \omega^{(0)} + \omega^{(2)}_{x_1 x_2} * * \langle E'_1 E'_2 \rangle + O\left(\left\langle E'^3 \right\rangle\right) = \omega^{(0)} + \Delta\omega + O\left(\left\langle E'^3 \right\rangle\right). \tag{95}$$

Using Eq. (91), the natural frequency variance reads:

$$\sigma_\omega^2 = \omega^{(1)}_{x_1} * \langle E'_1 E'_2 \rangle * \omega^{(1)}_{x_2} + O\left(\left\langle E'^3 \right\rangle\right) = \mathrm{Var}(\omega) + O\left(\left\langle E'^3 \right\rangle\right). \tag{96}$$

Apparently, up to the approximation of $\langle E'^3 \rangle$, $\langle \omega \rangle$ depends on the homogeneous frequency ($E = \langle E \rangle$) and on the second functional derivative of ω convoluted with the two-point correlation ($\langle E'_1 E'_2 \rangle$), while $\sigma^2{}_\omega$ depends on the first functional derivative of ω convoluted twice with $\langle E'_1 E'_2 \rangle$. Therefore, approximations for

the kth frequency mode are explicitly obtained once we have found the first and second functional derivatives. It is advantageous to normalize the kth frequency variance and average by the corresponding frequency mode of the homogeneous case:

$$\sigma_{\omega}^{2} = \frac{\mathrm{Var}(\omega)}{(\omega^{(0)})^{2}} + O\left(\left\langle E'^{3}\right\rangle\right) = \mathrm{Var}(\bar{\omega}) + O\left(\left\langle E'^{3}\right\rangle\right),$$
$$\left\langle \bar{\omega}'\right\rangle = \frac{\langle\omega\rangle - \omega^{(0)}}{\omega^{(0)}} = \Delta\bar{\omega} + O\left(\left\langle E'^{3}\right\rangle\right). \tag{97}$$

Calculating the first and second functional derivatives obtained in Section 3 and using the homogeneous solutions $\omega^{(0)}$, $U_x{}^{(0)}$ and $G_{x\xi}$ presented in Appendix A, we obtain for the C–C rod:

$$\mathrm{Var}(\bar{\omega}) = \cos^{2}(k\pi x_1) * \left\langle \bar{E}'_1 \bar{E}'_2\right\rangle * \cos^{2}(k\pi x_2), \tag{98}$$

$$\Delta\bar{\omega} = \cos(k\pi x_1) * \left(\left\langle \bar{E}'_1 \bar{E}'_2\right\rangle G_{x_2x_1,x_2x_1}\right) * \cos(k\pi x_2) - \frac{\mathrm{Var}(\bar{\omega})}{2}, \tag{99}$$

and for the S–S beam:

$$\mathrm{Var}(\bar{\omega}) = \sin^{2}(k\pi x_1) * \left\langle \bar{E}'_1 \bar{E}'_2\right\rangle * \sin^{2}(k\pi x_2), \tag{100}$$

$$\Delta\bar{\omega} = -\sin(k\pi x_1) * \left(\left\langle \bar{E}'_1 \bar{E}'_2\right\rangle G_{x_2x_1,x_2x_2x_1x_1}\right) * \sin(k\pi x_2) - \frac{\mathrm{Var}(\bar{\omega})}{2}. \tag{101}$$

Integration of Eqs. (98)–(101) using the two-point correlation function Eq. (94), yields analytical approximate expressions for the normalized variance and mean of ω as functions of the correlation length λ. For the C–C rod we obtain:

$$\mathrm{Var}(\bar{\omega}) = \frac{\bar{\sigma}_E^{2}\mathrm{e}^{-1/\lambda}\lambda}{4(1+4(k\pi\lambda)^2)^2}\begin{pmatrix} 8\lambda\left(1+2(k\pi\lambda)^2\right)^2 \\ +\mathrm{e}^{1/\lambda}\begin{pmatrix} 3-8\lambda+20(k\pi\lambda)^2 \\ -32(k\pi)^2\lambda^3 \\ +32(k\pi\lambda)^4-32(k\pi)^4\lambda^5 \end{pmatrix} \end{pmatrix}, \tag{102}$$

$$\Delta\bar{\omega} = \frac{\bar{\sigma}_E^{2}\mathrm{e}^{-1/\lambda}}{8(1+4(k\pi\lambda)^2)^3}\begin{pmatrix} 16(\lambda^2+4(k\pi)^2\lambda^4+12(k\pi)^4\lambda^6+16(k\pi)^6\lambda^8 \\ +\mathrm{e}^{1/\lambda}\begin{pmatrix} -4+11\lambda-4(4+11(k\pi)^2)\lambda^2+88(k\pi)^2\lambda^3 \\ -32(k\pi)^2(2+5(k\pi)^2)\lambda^4 \\ +240(k\pi)^4\lambda^5-192(1+(k\pi)^2)(k\pi)^4\lambda^6 \\ +256(k\pi)^6\lambda^7-256(k\pi)^6\lambda^8) \end{pmatrix} \end{pmatrix}, \tag{103}$$

and for the S–S beam:

$$\mathrm{Var}(\bar{\omega}) = \frac{-\bar{\sigma}_E^{2}\mathrm{e}^{-1/\lambda}\lambda}{4(1+4(k\pi\,\lambda)^2)^2}\left(-32(k\pi)^4+\mathrm{e}^{1/\lambda}\begin{pmatrix} -3-20(k\pi\lambda)^2 \\ +32(k\pi)^4(\lambda-1)^3\lambda^4 \\ +32(k\pi\lambda)^4-32(k\pi)^4\lambda^5 \end{pmatrix}\right), \tag{104}$$

$$\Delta\bar{\omega} = \frac{\bar{\sigma}_E^2}{4(1+4(k\pi\lambda)^2)^3}\left(\begin{array}{l} 8e^{-1/\lambda}(k\pi)^4\lambda^6(7+12(k\pi\lambda)^2) \\ +\dfrac{1}{(1+4(k\pi\lambda)^4)^2}\left(\begin{array}{l} 2+\lambda+24(k\pi\lambda)^2+9(k\pi)^2\lambda^3 \\ +110(k\pi\lambda)^4+46(k\pi)^4\lambda^5 \\ -56(k\pi)^4\lambda^6+316(k\pi\lambda)^6 \\ +92(k\pi)^6\lambda^7-96(k\pi)^6\lambda^8 \\ +856(k\pi\lambda)^8-88(k\pi)^8\lambda^9 \\ -448(k\pi)^8\lambda^{10}+1584(k\pi\lambda)^{10} \\ -224(k\pi)^{10}\lambda^{11}-768(k\pi)^{10}\lambda^{12} \\ +1792(k\pi\lambda)^{12}+128(k\pi)^{12}\lambda^{13} \\ -896(k\pi)^{12}\lambda^{14}+2816(k\pi\lambda)^{14} \\ +1539(k\pi)^{14}\lambda^{15}-1536(k\pi)^{14}\lambda^{16} \\ +(k\pi\lambda)(1+4(k\pi\lambda)^2)^3 \\ (1+4(k\pi\lambda)^4(1+4\lambda))\coth(k\pi) \end{array}\right) \end{array}\right). \tag{105}$$

While Hoshiya and Shah [7] and Ganesan and Shah [8] used only zero- and first-order terms and obtained natural frequency means which are identical to those for the homogeneous case, in this study the heterogeneity effect becomes apparent as more terms are taken into account. Eqs. (102)–(105) are plotted for different frequency modes in Fig. 3. The logarithmic scale helps in spanning the whole range of λ. Apparently, the heterogeneity effect on the mean natural frequencies is minimal for the fundamental mode, and may serve as a design tool. In addition, the same response to heterogeneity is observed for all modes, except for the frequency mean at $\lambda \ll 1$. It can be seen that the higher frequency modes are affected more as λ decreases, which means higher modes can "feel/see" the heterogeneity. Therefore, the same sensitivity to heterogeneity found in the deterministic case is exhibited here too.

Next, we wish to examine the effect of two different correlation functions on the frequency mean. For example, consider the function:

$$\langle E'x_1E'x_2\rangle = \bar{\sigma}_E^2 \exp\left(-\frac{\pi}{4}\left(\frac{x_2-x_1}{\lambda}\right)^2\right), \tag{106}$$

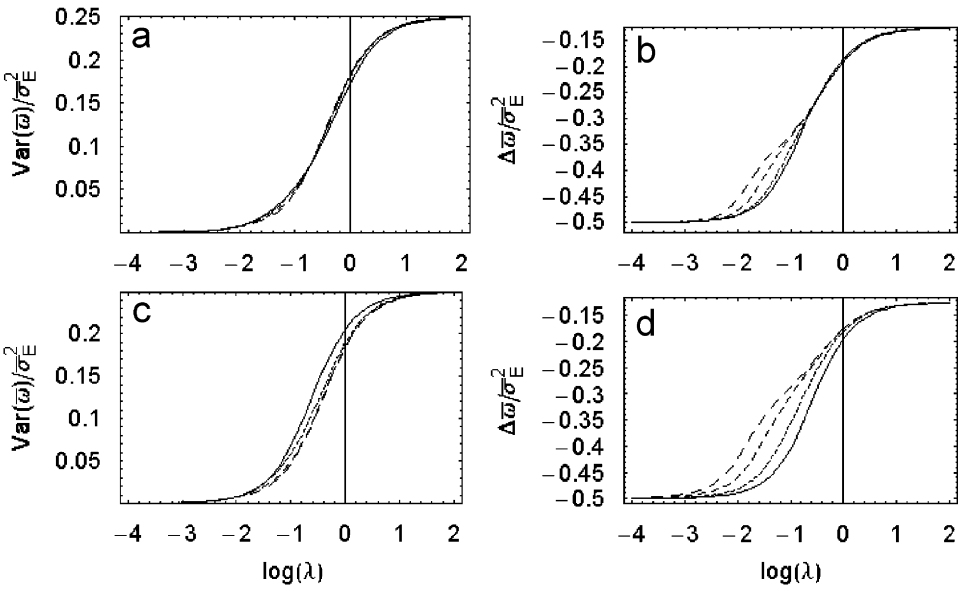

Fig. 3. (a) Rod's normalized frequency variance. (b) Rod's normalized frequency average. (c) Beam's normalized frequency variance. (d) Beam's normalized frequency average: ——, $k=1$: - - - - -, $k=2$: – – – –, $k=5$: — —, $k=10$.

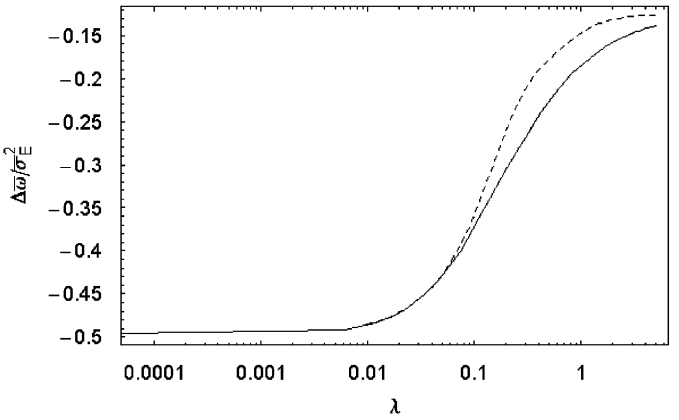

Fig. 4. Rod's fundamental frequency average calculated with the two point correlations: Eq. (94) ——, Eq. (106) – – –.

which describes a rather smooth change in E between neighbor grains. Note that choosing a different two-point correlation will not complicate the FPM. Eqs. (106) and (94) have the same correlation length, yet the first has higher correlation values in the region $\lambda > 0.1$. Consequently, as seen in Fig. 4, the rod's fundamental frequency mean is considerably different, especially in the region $\lambda > 0.1$.

For better insight into the mean and variance trend, it is worth looking at two extreme values of λ.

5.2. Large correlation lengths

Focusing on the range where λ is very large ($\lambda \gg 1$), the two-point correlation Eq. (94) can be written as:

$$\exp\left(-\frac{|x_2 - x_1|}{\lambda}\right) \cong 1 - \frac{|x_2 - x_1|}{\lambda}. \tag{107}$$

Thus, when $\lambda \gg 1$ an analytical approximation can be obtained as:

$$\mathrm{Var}(\bar{\omega}) \cong \bar{\sigma}_E^2 \left(\bar{\omega}_{x_1}^{(1)} * \left(1 - \frac{|x_2 - x_1|}{\lambda}\right) * \bar{\omega}_{x_2}^{(1)}\right), \tag{108}$$

$$\Delta\bar{\omega} \cong \bar{\sigma}_E^2 \left(\bar{\omega}_{x_1 x_2}^{(2)} * * \left(1 - \frac{|x_2 - x_1|}{\lambda}\right)\right). \tag{109}$$

Using Eqs. (108) and (109), the approximations for Eqs. (102)–(105) are:

$$\mathrm{Var}(\bar{\omega})|_{\lambda \gg 1} = \frac{\bar{\sigma}_E^2}{4}\left(1 - \frac{1}{\lambda}\left(\frac{1}{3} + \frac{3}{4k^2\pi^2}\right)\right), \tag{110}$$

$$\Delta\bar{\omega}|_{\lambda \gg 1} = -\frac{\bar{\sigma}_E^2}{8}\left(1 + \frac{1}{\lambda}\left(\frac{2}{3} - \frac{3}{4\pi^2 k^2}\right)\right), \tag{111}$$

$$\mathrm{Var}(\bar{\omega})|_{\lambda \gg 1} = \frac{\bar{\sigma}_E^2}{4}\left(1 + \frac{1}{\lambda}\left(\frac{15}{12k^2\pi^2} - \frac{1}{3}\right)\right), \tag{112}$$

$$\Delta\bar{\omega}|_{\lambda \gg 1} = -\frac{\bar{\sigma}_E^2}{8}\left(1 + \frac{1}{2\lambda}\left(1 + \frac{3}{(k\pi)^2}\right)\right). \tag{113}$$

Physically, a perfect modulus correlation length ($\lambda \to \infty$) means highly uniform material properties or alternatively an ensemble of rods or beams in which the modulus is homogeneous but may differ from one realization to another. Knowing that the homogeneous frequency is proportional to the modulus square root,

the exact normalized frequency variance and mean in this region are therefore equal to the normalized variance and mean of the modulus square root, respectively:

$$\langle \bar{\omega}' \rangle = \overline{\langle \sqrt{E'} \rangle}, \tag{114}$$

$$\bar{\sigma}_{\omega}^2 = \bar{\sigma}_{\sqrt{E}}^2. \tag{115}$$

This result is true for both beams and rods, and means that the frequency mean converges asymptotically to the exact solution of a homogeneous case with $E_h = \langle \sqrt{E} \rangle^2$:

$$\langle \omega \rangle|_{\lambda \to \infty} = \omega|_{E_h} = \omega|\langle \sqrt{E} \rangle^2. \tag{116}$$

Using Taylor series for expressing Eqs. (114) and (115) in terms of statistical information on E, we obtain:

$$\langle \bar{\omega}' \rangle \cong -\frac{1}{8}\bar{\sigma}_E^2 + O\left(E'^3\right), \tag{117}$$

$$\bar{\sigma}_{\omega}^2 \cong \frac{\bar{\sigma}_E^2}{4} + O\left(E'^3\right). \tag{118}$$

These results are confirmed by Fig. 3 and by Eqs. (110)–(113). The results show that in this region knowing the modulus statistical data are approximations to the frequency mean and variance. This means that the statistical data needed for the exact frequency mean and variance are the mean and variance of $\sqrt{E}$. Therefore, the modulus statistical data are the information needed for the exact mean and variance of the frequency square. Denoting $\beta = \omega^2$, up to a third-order approximation of $\langle E'^3 \rangle$ the following relations between ω and β are true:

$$\mathrm{Var}(\bar{\beta}) = 4\mathrm{Var}(\bar{\omega}), \tag{119}$$

$$\Delta\bar{\beta} = 2\Delta\bar{\omega} + \mathrm{Var}(\bar{\omega}). \tag{120}$$

Thus, for $\lambda \gg 1$ the mean and variance of β will converge to the values:

$$\Delta\bar{\beta} \to 0, \tag{121}$$

$$\mathrm{Var}(\bar{\beta}) \to \bar{\sigma}_E^2. \tag{122}$$

This shows that $\langle \beta \rangle$ converges asymptotically to the exact solution of a homogeneous case with $E_h = \langle E \rangle$.

5.3. Small correlation lengths

The range where λ is very small ($\lambda \ll 1$), means that the statistical correlation is limited to a small interval. As $\lambda \to 0$, all rods and beams will vibrate at the homogeneous natural frequency. Therefore, it is expected that the frequency variance will converge to zero. To obtain an analytical result for small λ, we define the small parameter:

$$h = |x_1 - x_2|, \tag{123}$$

which permits Taylor expansion of Eq. (96):

$$\bar{\sigma}_{\omega}^2 = \omega_{x_1}^{(1)} * \langle \bar{E}_1' \bar{E}_2' \rangle * \left(\omega_{x_1}^{(1)} + \omega_{x_1,x_1}^{(1)} h + \frac{1}{2}\omega_{x_1,x_1x_1}^{(1)} h^2 + \cdots \right). \tag{124}$$

Taking the first term of the expansion we have:

$$\mathrm{Var}(\omega) = \left(\omega_{x_1}^{(1)}\right)^2 * * \langle E_1' E_2' \rangle. \tag{125}$$

Calculating Eq. (125) for both the rods and the beams, we have:

$$\mathrm{Var}(\overline{\omega})\big|_{\lambda \ll 1} \cong \frac{3}{4}\lambda\overline{\sigma}_E^2. \tag{126}$$

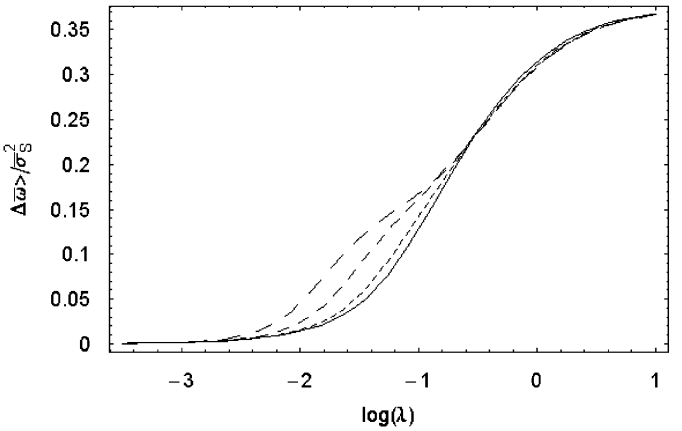

Fig. 5. Rod's normalized frequency average calculated by perturbation of S vs. log(λ): ——, $k=1$: ------, $k=2$: – – –, $k=5$: — —, $k=10$.

In addition, as $\lambda \to 0$ Eqs. (103) and (105) converge to:

$$\Delta\bar{\omega}|_{\lambda\to 0} = -\frac{1}{2}\bar{\sigma}_E^2. \tag{127}$$

Eqs. (126) and (127) are not confined to the exponential case, but hold for all morphologies with the same λ. It is clear that when $\lambda \to 0$, the effective uniform property is $S = 1/E$. Thus, the exact solution corresponds to:

$$\omega|_{S_h} = \omega|_{\langle S\rangle} = \frac{\pi k}{L\sqrt{\rho\langle S\rangle}}. \tag{128}$$

Using a Taylor series for expressing $\langle S\rangle$ in terms of statistical information on E, we obtain:

$$\langle S\rangle = \left\langle \frac{1}{E} \right\rangle \cong \frac{1}{\langle E\rangle}\left(1 - \bar{\sigma}_E^2 + \cdots\right). \tag{129}$$

Substitution of Eq. (129) in Eq. (128) yields:

$$\omega|_{\langle S\rangle} = \frac{\pi k}{L\sqrt{\rho\langle S\rangle}} \cong \omega|_{\langle E\rangle}\left(1 - \frac{1}{2}\bar{\sigma}_E^2\right). \tag{130}$$

It is seen that Eq. (130) verifies the values found through Eq. (127). Hence, $\langle S\rangle$ is the information needed for obtaining the exact solution at $\lambda \to 0$. Fig. 5 shows a rod's normalized frequency mean calculated through perturbation of S on a log(λ) scale. It can be seen that as $\lambda \to 0$, the solutions for all modes converge to zero (homogeneous frequency) as expected. Moreover, higher frequency modes are affected more as λ decreases, which means higher modes are sensitive to heterogeneity.

The above analysis demonstrates that the frequency accuracy depends on the available stochastic information (S, E or $\sqrt{E}$), on the size of λ, on the function about the perturbation is executed (E or S) and whether ω or ω^2 is of interest.

5.4. Effect of cross section variation in rods

Since the cross section parameter appears in both terms of the governing Eq. (13), and especially in view of the fact that homogeneous rods with different cross sections have the same natural frequencies, it is of interest to analyze the frequency variance and mean for varying cross section and uniform E and m. Note that Eq. (94) is used as the two-point correlation function.

5.4.1. Variance

The normalized frequency variance plotted on a log(λ) scale for the three first modes is shown in Fig. 6. This plot is of special interest, since in it the variance is exactly symmetric about the maximum point, which is not

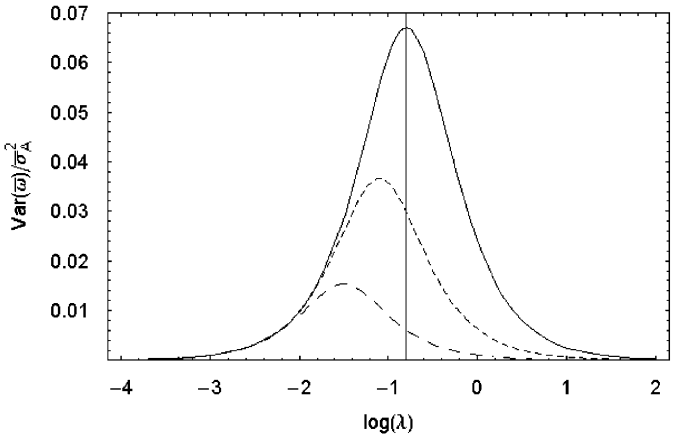

Fig. 6. Rod's normalized frequency variance calculated by perturbation of A vs. $\log(\lambda)$: ——, $k=1$: ------, $k=2$: – – –, $k=5$.

the case for a linear plot. This phenomenon cannot yet be explained and is currently being studied. Fig. 6 shows also that the normalized frequency variance approaches zero at very small and very large λ values for all modes, which means convergence to the solution of a homogeneous rod. This result fits the fact that the frequency of a homogeneous rod does not depend on the cross section. It can also be seen that the first mode serves as an upper bound for all higher modes, a fact of great importance to the designer who only needs to calculate the variance of the first mode, knowing that the response of all higher modes is smaller. The maximum variance, as well as its corresponding λ value, decrease as the mode number increases. This means that for high frequency modes, no matter how strong the cross section heterogeneity, the frequency variance will always be small. Fortunately, the maximum value of the normalized frequency variance and its corresponding λ value can be found analytically, as:

$$\lambda_{\mathrm{Max}}^{(k)} = \frac{1}{2k\pi}, \tag{131}$$

$$\left.\frac{\mathrm{Var}(\bar{\omega})}{\bar{\sigma}_A^2}\right|_{\lambda_{\mathrm{Max}}^{(k)}} = \frac{\exp(-2k\pi) + 2k\pi - 1}{8k^2\pi^2}. \tag{132}$$

Eq. (131) is directly related to the first cross section functional derivative through:

$$\langle A\rangle \bar{\omega}_{,A_1}\big|_{\langle A\rangle} = \cos(2\pi k x_1) = \cos\left(x_1/\lambda_{\mathrm{Max}}^{(k)}\right). \tag{133}$$

It can also be seen that for higher modes ($k \gg 1$) Eq. (132) reduces to:

$$\left.\frac{\mathrm{Var}(\bar{\omega})}{\bar{\sigma}_A^2}\right|_{\lambda_{\mathrm{Max}}^{(k)}} \to \frac{\lambda_{\mathrm{Max}}^{(k)}}{2}. \tag{134}$$

Eq. (133) brings out two important inherent characteristics of the first functional derivative. For the two-point correlation used, it reveals the correlation length in which the frequency variance reaches its maximum. Once the functional derivatives have been obtained, they are applicable for any morphology; thus, they act as the heterogeneity Green Function. For example, consider the case where the cross section morphology has a Dirac change at point x_1:

$$A_1' = \delta_{xx_1}, \tag{135}$$

the second term (first order) in the frequency series will then obviously be the first functional derivative at point x_1:

$$\langle A\rangle \bar{\omega}_{,A_1}\big|_{\langle A\rangle} * \delta_{xx_1} = \cos(2\pi k x_1) * \delta_{xx_1} = \cos(2\pi k x). \tag{136}$$

5.4.2. Mean

The normalized frequency mean which takes into account the cross section variation is shown in Fig. 7. In contrast to the frequency variance results, we see that here the first mode is a lower bound for all higher modes. Looking again at $\lambda \gg 1$, we see that all modes converge to zero, and coincide with the homogeneous solution which is independent of the cross section. This fits both the physics and variance results. Moreover, higher frequency modes ($k > 10$) reach this limit very quickly, meaning that they are less affected by heterogeneity. This result is also supported by the frequency variance results (Fig. 6). When $\lambda \to 0$, all modes converge to:

$$\Delta\bar{\omega}|_{\lambda\to 0} = -\frac{1}{2}\bar{\sigma}_A^2. \tag{137}$$

Using an elementary expansion (three terms) for a homogeneous effective property (say $\theta(A)$) in terms of cross section statistical data, it can be proved that:

$$\Delta\bar{\omega}|_{\langle\theta\rangle} \cong -\frac{1}{2}\bar{\sigma}_A^2, \quad \theta = \frac{1}{\sqrt{A}}. \tag{138}$$

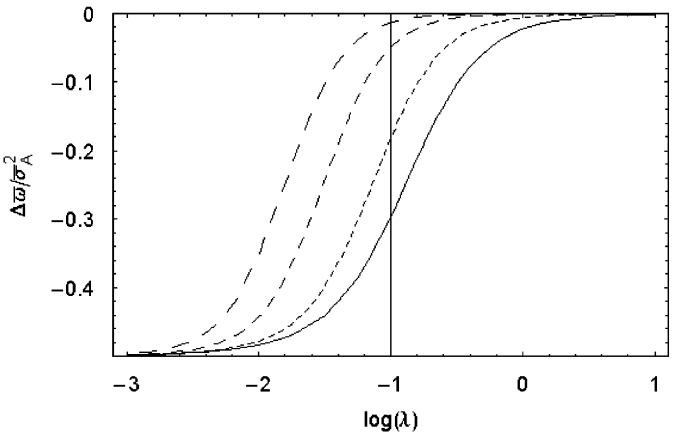

Fig. 7. Rod's normalized frequency average calculated by perturbation of A vs. $\log(\lambda)$: ——, $k = 1$: - - - - -, $k = 2$: – – –, $k = 5$: — —, $k = 10$.

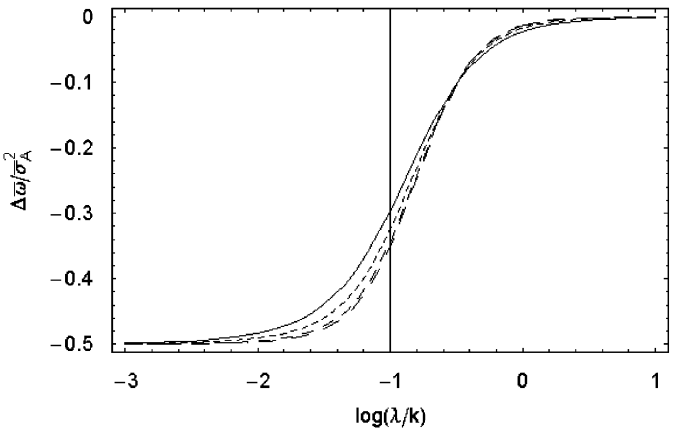

Fig. 8. Rod's normalized frequency average calculated by perturbation of A vs. $\log(\lambda/k)$: ——, $k = 1$: - - - - - -, $k = 2$: – – –, $k = 5$: — —, $k = 10$.

It shows that for small values of λ the important statistical data property is $1/\sqrt{A}$. This result is in conflict with intuition, because as $\lambda \to 0$ there is an ensemble of rods which in effect vibrate with the same homogeneous frequency, although the latter does not depend on the cross section. This unexplained result is still being studied. Fig. 8 shows that when $\Delta\omega$ is plotted on a $\log(\lambda/k)$ scale all curves converge. This result indicates that all modes will have the same response to the cross section heterogeneity as long as the mode wave length (k) is of the order of λ.

6. Conclusions

Several important advantages of the FPM are shown:

1. The FPM is analytical and provides a physical insight into the effect of heterogeneity of each frequency order.
2. The functional derivatives are generic results of solving each perturbation order and do not depend on prescribed shape functions.
3. Once the functional derivatives have been found, the solution for any morphology is obtained by direct integration without re-solving the differential equation for each heterogeneity separately. Therefore, the functional derivatives serve as the Green Function for Morphology.
4. The same functional derivatives can be used for reliability analysis. It should be mentioned that functional derivatives are already available as routines in commercial programs such as Mathematica.

For the deterministic case, we compared the FPM natural frequencies and mode shapes with exact solutions for a number of non-uniformities in material and geometry. It is shown that the relative error is small even for large variations. In addition, the natural frequencies of both the deterministic and stochastic cases are sensitive to heterogeneity. The strongest sensitivity is observed when the frequency mode has a ''wave length'' of the order of the heterogeneity characteristic length λ.

For the stochastic case, we obtained analytical approximate solutions for the mean and variance of the natural frequencies. The solution converges to its exact counterparts at both morphology regions $\lambda \to 0$ and $\lambda \to \infty$. It was also shown that the solution accuracy depends on the size of λ. In addition:

1. The stochastic information used/given. Namely, at $\lambda \gg 1$ the stochastic information on $\sqrt{E}$ is needed for exact solution of $\langle \omega \rangle$. However, in the same λ region information on E is required for the exact value of $\langle \omega^2 \rangle$.
2. The frequency accuracy are strongly depends on the material property (E or $S = \mathrm{E}^{-1}$) about which the FPM is executed. It was shown how S is the appropriate property for $\lambda \ll 1$ and $\sqrt{E}$ is for $\lambda \gg 1$.

For future study it is important to find the natural frequencies for non-uniform 3-D structures as well as for structures with non-negligible damping.

Acknowledgments

This study was partially supported by the Israeli Science Foundation and the B. and N. Ginsberg research fund of the Technion.

Appendix A

Homogeneous natural frequencies and mode shapes and the Green Function for various boundary conditions are introduced.

C–C rod

$$\begin{aligned} &U_x^{(0)}\big|_{x=0} = U_x^{(0)}\big|_{x=1} = 0, \quad \left(U_x^{(0)}\right)^2 * 1_x = 1, \\ &U_x^{(0)} = \sqrt{2}\sin(k\pi x), \qquad \beta = k\pi. \end{aligned} \tag{A.1}$$

$$G_{x\xi} = \begin{cases} \dfrac{1}{2k^2\pi^2}\begin{pmatrix} 2k\pi x\,\cos(k\pi x)\sin(k\pi\xi) + \sin(k\pi x) \\ (2k\pi(-1+\xi)\cos(k\pi\xi) - \sin(k\pi\xi) \end{pmatrix}, & x<\xi, \\ \dfrac{1}{2k^2\pi^2}\begin{pmatrix} 2k\pi x(-1+x)\cos(k\pi x)\sin(k\pi\xi) \\ +\sin(k\pi x)(2k\pi\cos(k\pi\xi) - \sin(k\pi\xi) \end{pmatrix}, & x>\xi. \end{cases} \tag{A.2}$$

C–F rod

$$\begin{aligned} &U_x^{(0)}\big|_{x=0} = U_{x,x}^{(0)}\big|_{x=1} = 0, \quad \left(U_x^{(0)}\right)^2 * 1_x = 1, \\ &U_x^{(0)} = \sqrt{2}\sin(\beta x), \qquad \beta = \frac{(2k-1)\pi}{2}. \end{aligned} \tag{A.3}$$

$$G_{x\xi}\begin{cases} \dfrac{4\sin((2k-1)\pi\xi/2)^2}{(\pi-2k\pi)^2(\cos((2k-1)\pi\xi)-1)}\begin{pmatrix} -(2k-1)\pi(\xi-1)\cos((2k-1)\pi\xi/2) \\ \sin((2k-1)\pi x/2) + \sin((2k-1)\pi\xi/2) \\ \begin{pmatrix} (2k-1)\pi x\cos((2k-1)\pi x/2) \\ +\sin((2k-1)\pi x/2) \end{pmatrix} \end{pmatrix} & x<\xi \\ \dfrac{1}{(\pi-2k\pi)^2}\begin{pmatrix} 2(2k-1)\pi(x-1)\cos((2k-1)\pi x/2) \\ \sin((2k-1)\pi\xi/2) + 2\,\sin((2k-1)\pi x/2) \\ (2k-1)\pi\xi\cos((2k-1)\pi\xi/2) + \sin((2k-1)\pi\xi/2) \end{pmatrix} & x>\xi \end{cases} \tag{A.4}$$

S–S beam

$$\begin{aligned} &U_x^{(0)}\big|_{x=0} = U_{x,xx}^{(0)}\big|_{x=0} = U_{x,xx}^{(0)}\big|_{x=1} = U_x^{(0)}\big|_{x=1} = 0, \quad \left(U_x^{(0)}\right)^2 * 1_x = 1, \\ &U_x^{(0)} = \sqrt{2}\sin(k\pi x), \qquad \beta = k\pi. \end{aligned} \tag{A.5}$$

$$G_{x\xi} = \begin{cases} \dfrac{1}{4k^2\pi^2}\begin{pmatrix} -2k\pi x\cos(k\pi x)\sin(k\pi\xi) + (-2k\pi(-1+\xi)\cos(k\pi\xi) \\ +3\sin(k\pi\xi))\sin(k\pi x) \\ +2k\pi\mathrm{csch}(k\pi)\sinh(k\pi(-1+\xi))\sinh(k\pi x) \end{pmatrix}, & x<\xi, \\ \dfrac{1}{4k^4\pi^4}\begin{pmatrix} -2k\pi(-1+x)\cos(k\pi x)\sin(k\pi\xi) \\ +(-2k\pi\xi\,\cos(k\pi\xi) + 3\sin(k\pi\xi))\sin(k\pi x) \\ +2k\pi\mathrm{csch}(k\pi)\sinh(k\pi(-1+x))\sinh(k\pi\xi) \end{pmatrix}, & x>\xi. \end{cases} \tag{A.6}$$

References

[1] M. Eisenberger, Exact longitudinal vibration frequencies of a variable cross section, *Applied Acoustic* 34 (1991) 123–130.
[2] S. Abrate, Vibration of non-uniform rods and beams, *Journal of Sound and Vibration* 185 (4) (1995) 703–716.
[3] B.M. Kumar, R.I. Sujith, Exact solutions for the longitudinal vibrations of non-uniform rods, *Journal of Sound and Vibration* 207 (5) (1997) 721–729.

[4] C.O. Horgan, A.M. Chan, Vibration of inhomogeneous strings rods and membranes, *Journal of Sound and Vibration* 225 (3) (1999) 503–513.
[5] I. Elishakoff, *Eigenvalues of Inhomogeneous Structures: Unusual Closed-Form Solutions*, CRC Press, Boca Raton, 2005.
[6] I. Elishakoff, S. Candan, Apparently first closed-form solution for vibrating: inhomogeneous beams, *International Journal of Solids and Structures* 38 (2001) 3411–3441.
[7] M. Hoshiya, H.C. Shah, Free vibration of stochastic beam-column, *Journal of the Engineering Mechanics Division* 4 (1971) 1239–1255.
[8] R. Ganesan, V.K. Kowda, Free vibration of composite beam-columns with stochastic material and geometrical properties subjected to axial loads, *Journal of Reinforced Plastics and Composites* 24 (2005) 69–91.
[9] R. Vaicaitis, Free vibrations of beam with random characteristics, *Journal of Sound and Vibration* 35 (1) (1974) 13–21.
[10] C.S. Manohar, A.J. Keane, Axial vibrations of stochastic rod, *Journal of Sound and Vibration* 165 (2) (1993) 341–359.
[11] E. Altus, Statistical modeling of heterogeneous microbeams, *International Journal of Solids and Structures* 38 (34-35) (2001) 5915–5934.
[12] E. Altus, S. Givli, Strength reliability of statistically heterogeneous microbeams, *International Journal of Solids and Structures* 40 (9) (2003) 2069–2083.
[13] E. Altus, E. Totry, Buckling of stochastically heterogeneous beams, using a functional perturbation method, *International Journal of Solids and Structures* 40 (23) (2003) 6547–6565.
[14] M. Beran, *Statistical Continuum Mechanics*, Inter Publisher, McGraw-Hill Book Company, New York, 1968, pp. 1–141.
[15] S. Timoshenko, D.H. Young, W. Weaver Jr., *Vibration Problems in Engineering*, fourth ed., New York, McGraw-Hill, 1974, pp. 363–459.
[16] V.I. Smirnov, *A Course of Higher Mathematics*, Vol. 1, New York, Pergamon Press, 1964.
[17] I. Stakgold, *Boundary Value Problems of Mathematical Physics*, Vol. 1, New York, Collier-Macmillan, 1967.